

Supplementary data

Incorporation of a Z-scheme AgI/Ag₆Si₂O₇ heterojunction to PET fabric for efficient and repeatable photocatalytic dye degradation

Lili Wang¹, Lei Chen¹, Mengyao Tang¹, Shoujie Jiang^{1,2}, Dawei Gao^{1*}

1 College of Textiles and Clothes, Yancheng Institute of Technology, Yancheng, 224051, China

2 School of Textile Science and Engineering, Xi'an Polytechnic University, Xi'an 710048, China

Corresponding author:

gaodawei@ycit.edu.cn (D. Gao)

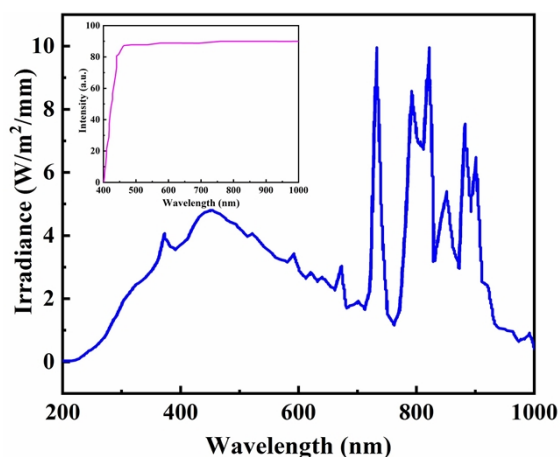


Figure S1 Xe spectrum produced by Xenon lamp and transmittance of the cut-off film (Inserted).

Figure S2 SEM image of PET.

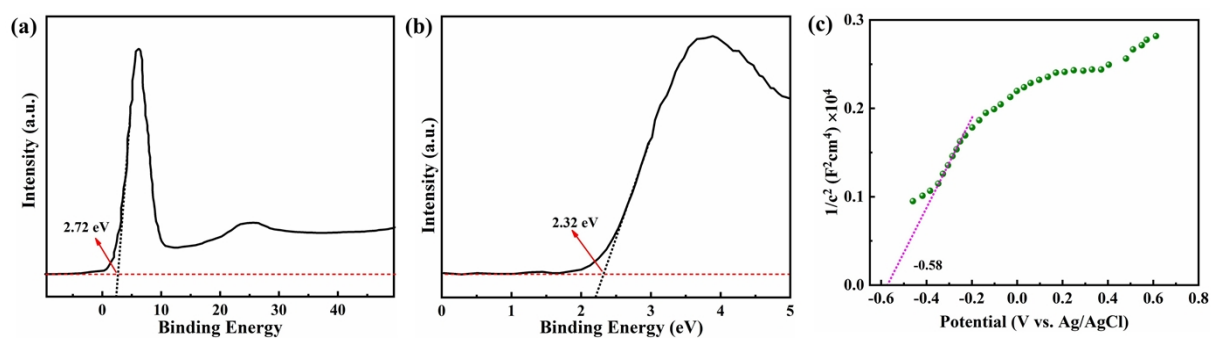


Figure S3 Valence band XPS spectra of $\text{Ag}_6\text{Si}_2\text{O}_7/\text{PET}$ (a) and AgI/PET (b), Mott-Schottky plots of AgI/PET (c).

Figure S3 showed that the VB of $\text{Ag}_6\text{Si}_2\text{O}_7$ was 2.72 V vs NHE and its CB can be calculated to be 1.44 V vs NHE (Figure S3a). The band gap structure of AgI was first

determined through XPS spectra of valence band (Figure S3b) and Mott-Schottky plots (Figure S3c). Positive slopes for Mott-Schottky plots indicated that AgI verified n-type semiconductor characteristics. Through the extrapolation of the x intercept in the Mott-Schottky curves, the flat-band potential of AgI could be evaluated to be -0.38 V (vs NHE). The valence XPS spectra could be used to check the energy gap from Fermi level (E_f) to the valence band top of semiconductors. The valence band top positions of AgI was 2.32 eV below the E_f . And the E_f was close to flatband potential for n-type semiconductor. Combined with the E_g value, the VB and CB of AgI was 1.94 eV and -0.76 eV, respectively.”

Figure S4 Photodegradation of MO, RhB and PhOH of AgI/Ag₆Si₂O₇/PET(5) under visible-light irradiation.

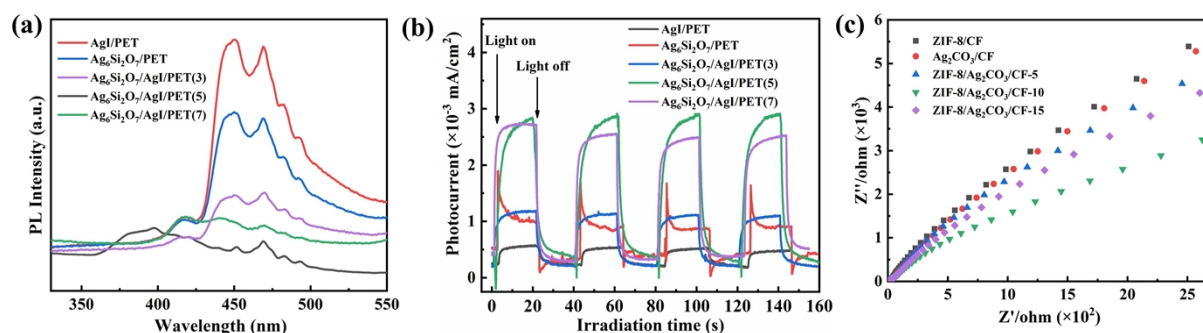


Figure S5 The PL spectra (a), transient photocurrent response (b) and EIS plots (c) of the as-prepared samples.

Figure S6 Nitrogen adsorption-desorption isotherm of $\text{Ag}_6\text{Si}_2\text{O}_7/\text{PET}$, AgI/PET and $\text{AgI}/\text{Ag}_6\text{Si}_2\text{O}_7/\text{PET}(5)$.

Table S1 BET surface area and pore size of $\text{Ag}_6\text{Si}_2\text{O}_7/\text{PET}$, AgI/PET and $\text{AgI}/\text{Ag}_6\text{Si}_2\text{O}_7/\text{PET}(5)$

| Samples | S_{BET} (m^2/g) | Pore Volume (cm^3/g) | Pore size (nm) |
|---|--|--|----------------|
| $\text{Ag}_6\text{Si}_2\text{O}_7/\text{PET}$ | 1.754 | 0.004 | 3.432 |
| AgI/PET | 28.347 | 0.115 | 1.466 |
| $\text{AgI}/\text{Ag}_6\text{Si}_2\text{O}_7/\text{PET}(5)$ | 5.746 | 0.022 | 1.849 |

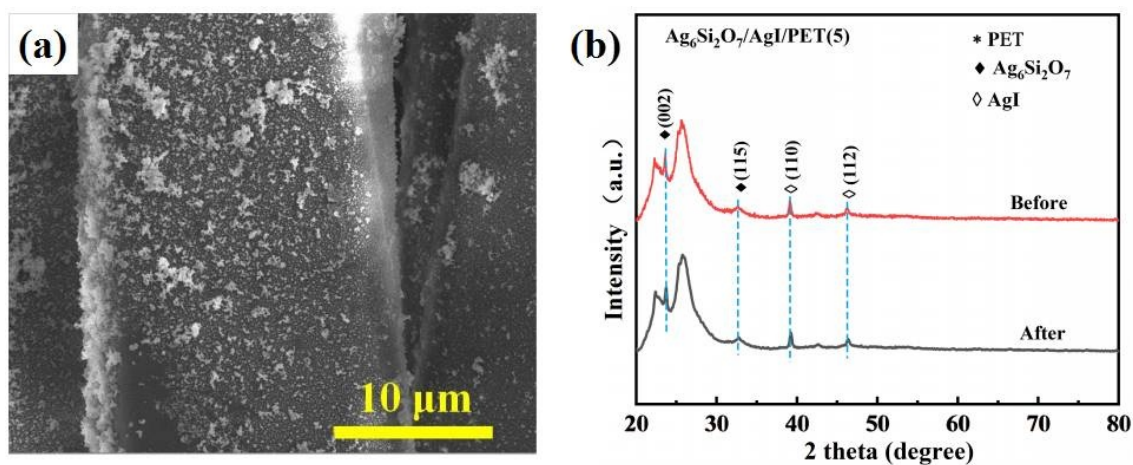


Figure S7 SEM image (a) and XRD patterns (b) of $\text{AgI}/\text{Ag}_6\text{Si}_2\text{O}_7/\text{PET}(5)$ after 5 cycles' photocatalysis.

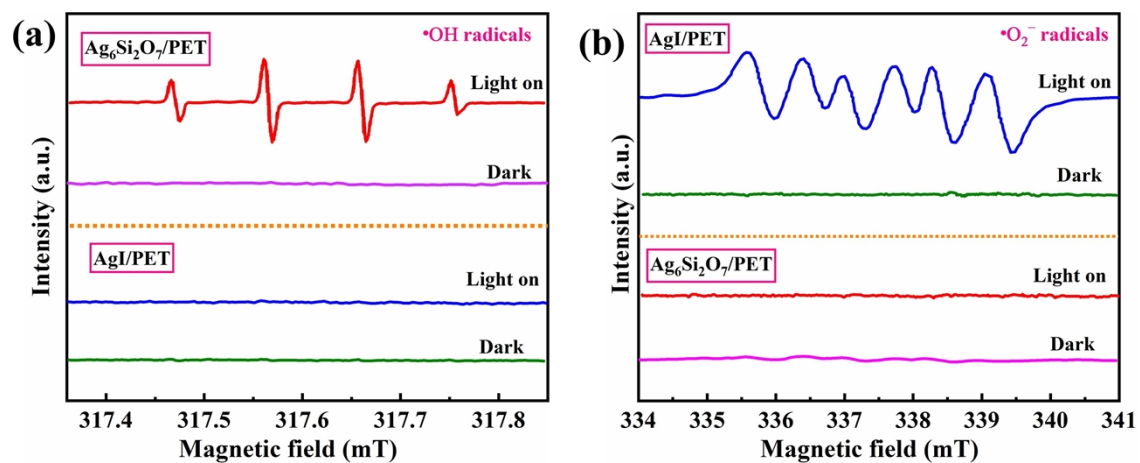


Figure S8 The ESR signals of $\cdot\text{OH}$ (a) and $\cdot\text{O}_2^-$ (b) of $\text{AgI}/\text{Ag}_6\text{Si}_2\text{O}_7/\text{PET}$ and AgI/PET .